

PITHA 09/20
SFB/CPP-09-81
March 10, 2019

NLO QED Corrections to Hard-Bremsstrahlung Emission in Bhabha Scattering

STEFANO ACTIS *

*Institut für Theoretische Physik E, RWTH Aachen University,
D-52056 Aachen, Germany*

PIERPAOLO MASTROLIA †

*Theory Group, Physics Department, CERN,
CH-1211 Geneva 23, Switzerland*

GIOVANNI OSSOLA ‡

*Physics Department, New York City College of Technology,
300 Jay Street, Brooklyn NY 11201, USA*

In this paper we present a numerical implementation of the one-loop QED corrections to the hard-bremsstrahlung process $e^-e^+ \rightarrow e^-e^+\gamma$. These corrections can be included in the Monte Carlo event generators employed for simulating Bhabha scattering events at low-energy high-luminosity electron-positron colliders. The calculation is performed by employing the reduction method developed by Ossola, Papadopoulos and Pittau. Our results are implemented in a modular code for the numerical evaluation of the scattering amplitudes for any given phase-space point. In a similar way, we also evaluate the one-loop QED corrections to $e^-e^+ \rightarrow \mu^-\mu^+\gamma$, which represents an interesting application of the method in the presence of two different mass scales in the loops.

Keywords: NLO computations, QED, hard bremsstrahlung

PACS classification: 12.20.Ds, 13.66.Jn

*actis@physik.rwth-aachen.de

†Pierpaolo.Mastrolia@cern.ch

‡gossola@citytech.cuny.edu

1 Introduction

Bhabha scattering ($e^-e^+ \rightarrow e^-e^+$) is the process employed as a luminosity candle at all electron-positron colliders. In particular, at high-energy colliders such as LEP, the luminosity was measured by considering Bhabha scattering events at small scattering angles. At high-luminosity meson factories (DAΦNE, CESR, etc.), operating at a center-of-mass energy of 1–10 GeV, the luminosity is determined by analyzing large-angle Bhabha scattering events. In both cases, the Bhabha scattering cross section is large and dominated by electromagnetic interactions. Therefore, by employing the techniques of perturbative QED, it is possible to predict the cross section with high accuracy. This is extremely relevant, since the theoretical uncertainty affecting the prediction for the cross section directly relates to the accuracy for the determination of the luminosity of a given collider.

For phenomenological studies and luminosity determinations, fixed-order calculations of the Bhabha scattering cross section need to be interfaced with sophisticated Monte Carlo (MC) generators, which take into account realistic experimental cuts and the geometry of the detectors. Experimental analyses rely on programs such as BABAYAGA@NLO [1], MCGPJ [2] and BH-WIDE [3], which include next-to-leading order (NLO) corrections and effects related to multiple photon emission. The three generators mentioned above agree within 0.1% for integrated cross sections and within 1% for distributions as shown in Ref. [4].

On the theoretical side, NLO corrections to $e^-e^+ \rightarrow e^-e^+$ are well under control. In particular, one-loop corrections in the full Standard Model were calculated long ago [5].

NNLO QED corrections to the Bhabha scattering cross section play a key role in establishing the accuracy of current MC generators and, eventually, in improving it below 0.1% as it might be required by electron-positron colliders of the next generation, such as the planned International Linear Collider.

It is possible to subdivide NNLO corrections in three different sets: *i*) two-loop corrections to the process $e^-e^+ \rightarrow e^-e^+$; *ii*) one-loop corrections including a single hard photon in addition to the outgoing electron-positron pair; *iii*) real corrections with two hard photons or a hard electron-positron pair in the final state. Although some of the diagrams belonging to the sets *i*) and *ii*) are infrared divergent, it is possible in both cases to isolate a class of soft-photon corrections which, when added to the corresponding set of loop corrections, makes the sum infrared finite.

The calculation of the two-loop corrections belonging to set *i*) was completed only recently [6–9]. Two-photon corrections of class *iii*) can be computed with any of the existing publicly available tree-level event generators and are safely under control. However, virtual and real corrections involving one additional hard photon in the final state (class *ii*) are not completely known. Partial results are available for small-angle Bhabha scattering [10] and s -channel annihilation processes at large angles [11].

The aim of this letter is to present the calculation of the one-loop corrections belonging to the set *ii*). Specifically, we realized a FORTRAN 95 code which allows for evaluating numerically at fixed phase-space points the one-loop QED corrections to the process $e^-e^+ \rightarrow e^-e^+\gamma$ retaining a finite electron mass; here γ denotes a photon with an energy larger than a given cut-off threshold. The calculation was carried out by employing the Ossola-Papadopoulos-Pittau (OPP) method [12, 13], based on a reduction of the tensor integrals performed at the integrand level [14].

As a by-product, we computed the one-loop QED corrections to the annihilation process $e^-e^+ \rightarrow \mu^-\mu^+\gamma$. This reaction involves an additional mass scale and represents an important background for the determination of the pion form factor and provides an independent calibration for a measurement of the hadronic production cross section. Note that a partial implementation of

NLO radiative corrections to the latter process is currently available in PHOKHARA [15].

The paper is organized as follows. In Section 2 we set our notation and conventions and briefly describe the computational technique which we employed. In Section 3 we provide numerical results for specific benchmark phase space points. Section 4 contains our conclusions, including comments on the numerical stability of the results and on the computer time required by the calculation.

2 Calculation of Radiative Corrections

2.1 Conventions and Leading Order Cross Section

We consider the hard-bremsstrahlung processes

$$e^-(k_1) + e^+(k_2) \rightarrow f^-(k_3) + f^+(k_4) + \gamma(k_5), \quad f = e, \mu, \quad (1)$$

where k_1 and k_2 denote the momenta of the colliding electron and positron, k_3 and k_4 stand for the momenta of the outgoing fermion and anti-fermion, and k_5 is the momentum of the outgoing hard photon. The particle momenta obey the mass-shell conditions $k_1^2 = k_2^2 = m_e^2$, $k_3^2 = k_4^2 = m_f^2$ and $k_5^2 = 0$. The kinematics is described by five independent invariants, which can be chosen among the six quantities

$$s = (k_1 + k_2)^2 = 4E^2, \quad s' = (k_3 + k_4)^2, \quad t_{ij} = (k_i - k_j)^2, \quad i = 1, 2, \quad j = 3, 4. \quad (2)$$

Here E indicates the beam energy in the center-of-mass frame.

The unpolarized leading order (LO) cross section can be written as

$$d\sigma_{\text{LO}} = \frac{1}{2\sqrt{s(s-4m_e^2)}} dR_3 \frac{1}{4} \sum_{\text{spins}} |\mathcal{M}_{\text{tree}}|^2, \quad (3)$$

where $\mathcal{M}_{\text{tree}}$ represents the tree-level amplitude. In the context of pure QED, the latter originates from the Feynman diagrams shown in Fig. 1. The n -particle phase space is defined by

$$dR_n = \left(\prod_{i=3}^{n+2} \frac{d^3 k_i}{(2\pi)^3 2E_i} \right) (2\pi)^4 \delta^{(4)} \left(k_1 + k_2 - \sum_{j=3}^{n+2} k_j \right). \quad (4)$$

The LO cross section for real-photon emission of Eq. (1) was computed long ago in Refs. [16] and can be written in a compact way in the ultrarelativistic limit [17]. Since these relations can be employed for checks, we report their expressions. Results are more conveniently expressed in terms of the kinematic invariants of Eq. (2) and of the variables $k_{i5} = k_i \cdot k_5$, with $i = 1, \dots, 4$, as

$$\frac{1}{4} \sum_{\text{spins}} |\mathcal{M}_{\text{tree}}|^2 = (4\pi\alpha)^3 \mathcal{T} \left(\frac{s}{k_{15}k_{25}} + \frac{s'}{k_{35}k_{45}} - \frac{t_{13}}{k_{15}k_{35}} - \frac{t_{24}}{k_{25}k_{45}} + \frac{t_{14}}{k_{15}k_{45}} + \frac{t_{23}}{k_{25}k_{35}} \right), \quad (5)$$

where the function \mathcal{T} depends on the final-state fermions. For the process $e^-e^+ \rightarrow e^-e^+\gamma$ one finds

$$\mathcal{T} = \frac{1}{ss't_{13}t_{24}} [ss'(s^2 + s'^2) + t_{13}t_{24}(t_{13}^2 + t_{24}^2) + t_{14}t_{23}(t_{14}^2 + t_{23}^2)], \quad (6)$$

while for the case $e^-e^+ \rightarrow \mu^-\mu^+\gamma$ the function \mathcal{T} is

$$\mathcal{T} = \frac{1}{ss'} (t_{13}^2 + t_{14}^2 + t_{23}^2 + t_{24}^2). \quad (7)$$

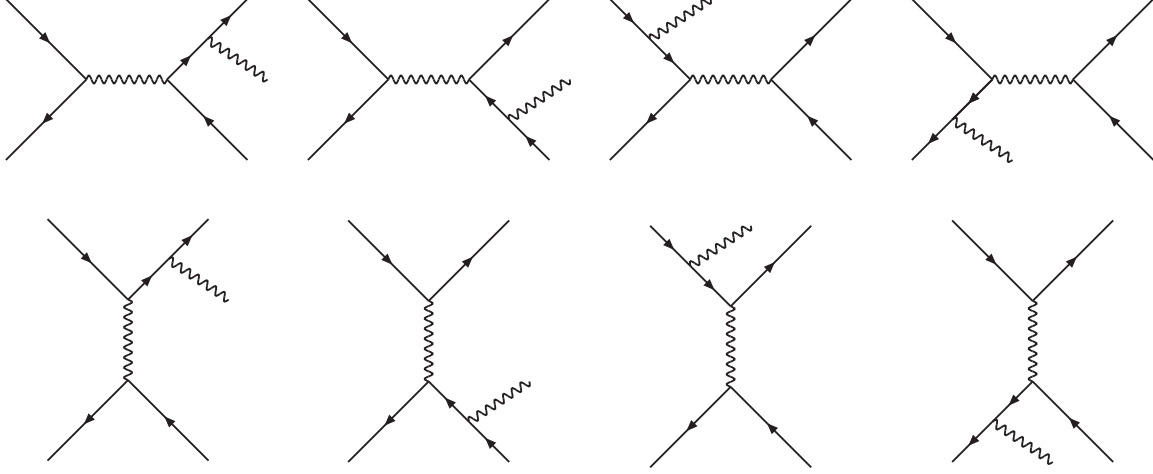


Figure 1: QED tree-level diagrams for $e^-e^+ \rightarrow e^-e^+\gamma$ (full set) and $e^-e^+ \rightarrow \mu^-\mu^+\gamma$ (first line). Here and in the following, particles on the left side of the diagrams are considered incoming, particles on the right side of the diagrams are outgoing.

2.2 Virtual Corrections

The one-loop corrections to the two scattering processes studied in this work involve a relatively limited number of Feynman diagrams: the package QGRAF [18] generates 38 one-loop diagrams for the process $e^-e^+ \rightarrow \mu^-\mu^+\gamma$ and 76 diagrams for the process $e^-e^+ \rightarrow e^-e^+\gamma$. Representative graphs are shown in Fig. 2; note that due to Furry's theorem, diagrams of class 2c cancel in the sum.

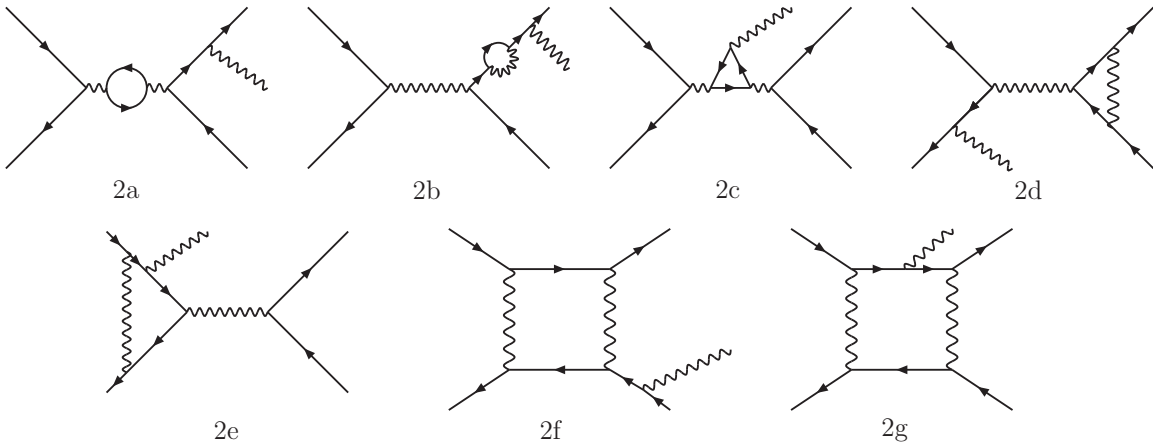


Figure 2: Representative one-loop diagrams for $e^-e^+ \rightarrow e^-e^+\gamma$.

As can be seen from Fig. 2, the calculation of the complete one-loop corrections requires the evaluation of pentagon graphs, the most challenging and time consuming part of this calculation.

It is well known that any four-dimensional one-loop amplitude can be written as a linear com-

combination of scalar box, triangle, bubble and tadpole integrals, whose analytic expressions were obtained in the seminal paper by 't Hooft and Veltman [19]. The coefficients multiplying the one-loop integrals are ratios of polynomials in the kinematical invariants. These coefficients have been traditionally determined by means of the Passarino-Veltman (PV) reduction method [20]. However, for processes with more than four external legs, a straightforward application of the PV reduction can generate very large expressions involving inverse Gram determinants. The latter can be a source of numerical instabilities.

In recent years, a significant amount of work was devoted to the evaluation of one-loop amplitudes for processes with five or more external legs (for a review see [21]). Besides improvements on standard techniques, where a tensor reduction is explicitly performed, new numerical and analytical developments have emerged. Both directions have been successfully pursued and have led to impressive results. In particular, in the last few months, very challenging LHC calculations involving four particles in the final state have been completed [22, 23].

In the present paper, we evaluate the one-loop corrections to the processes $e^-e^+ \rightarrow \mu^-\mu^+\gamma$ and $e^-e^+ \rightarrow e^-e^+\gamma$ by means of the OPP reduction method [12, 13]. Following the OPP approach, we perform the reduction numerically for each phase space point. The one-loop amplitude generated by QGRAF was processed with FORM [24] routines in order to produce a FORTRAN 95 output. The latter was then used as input for the two computer implementations of the OPP technique which we employed [25, 26].

The one-loop corrections to the cross section can be written as

$$d\sigma_{\text{NLO}}^{\text{V}} = \frac{1}{2\sqrt{s(s-4m_e^2)}} dR_3 \frac{1}{4} \sum_{\text{spins}} 2\text{Re}(\mathcal{M}_{1\text{-loop}}\mathcal{M}_{\text{tree}}^*), \quad (8)$$

where, in the spirit of the OPP reduction technique, the interference of the one-loop amplitude $\mathcal{M}_{1\text{-loop}}$ with the complex-conjugate tree-level amplitude $\mathcal{M}_{\text{tree}}^*$, evaluated in dimensional regularization, can be split as follows

$$\frac{1}{4} \sum_{\text{spins}} 2\text{Re}(\mathcal{M}_{1\text{-loop}}\mathcal{M}_{\text{tree}}^*) = \mathcal{CC}_4 + \mathcal{R}_1 + \mathcal{R}_2 + \mathcal{UV}_{ct}. \quad (9)$$

Here \mathcal{CC}_4 denotes the cut-constructible four-dimensional part of the result, written as a linear combinations of scalar boxes, triangles, bubbles and tadpoles, $\mathcal{R}_1 + \mathcal{R}_2$ stands for the so-called rational part and \mathcal{UV}_{ct} summarizes all contributions induced by the ultraviolet counterterms. Note that throughout our computation we have used strictly four-dimensional external momenta.

The rational part was split into two components, \mathcal{R}_1 and \mathcal{R}_2 , as explained in Ref. [27]. The integrand connected with a m -point one-loop Feynman graph can be written as follows:

$$\bar{A}(\bar{q}) = \frac{\bar{N}(\bar{q})}{\bar{D}_0 \dots \bar{D}_{m-1}}, \quad \bar{D}_i = (\bar{q} + p_i)^2 - m_i^2. \quad (10)$$

In the equation above a bar denotes objects living in $d = 4 - 2\epsilon$ space-time dimensions, q is the loop momentum, p_i are linear combinations of the external four-dimensional momenta and m_i stand for the masses of the internal legs. The numerator $\bar{N}(\bar{q})$ can be split in a four-dimensional and an ϵ -dimensional part (indicated by a tilde): $\bar{N}(\bar{q}) = N_1(q) + \tilde{N}_2(\bar{q})$. The four-dimensional numerator $N_1(q)$ is then expanded in terms of four-dimensional denominators D_i [12]: the mismatch in dimensionality between the denominators D_i and the d -dimensional propagators \bar{D}_i gives origin to the \mathcal{R}_1 term in Eq. (9). The \mathcal{R}_2 component, instead, stems from the overlap between $\tilde{N}_2(\bar{q})$

and the ultraviolet poles of one-loop integrals, and can be evaluated in QED by employing the ad-hoc counterterm-like Feynman rules presented in Ref. [27]. Note that the overlap between the ϵ -dimensional numerator $\tilde{N}_2(\bar{q})$ and the infrared poles of one-loop integrals can be safely neglected from the very beginning as proven in Appendix A of Ref. [28].

We carried out the ultraviolet renormalization in the on-mass-shell scheme: the renormalized charge is chosen to be equal to the value of the electromagnetic coupling, as measured in Thomson scattering, at all orders in perturbation theory; the squared fermion masses are identified with the real parts of the poles of the Dyson-resummed propagators; field-renormalization constants cancel by definition external wave-function corrections.

Throughout our computation we have retained the full dependence on the fermion masses, introducing in particular the appropriate mass-counterterm diagrams, depicted in Fig. 3.



Figure 3: Representative mass-counterterm diagrams for $e^-e^+ \rightarrow e^-e^+\gamma$. Black dots stand for mass-counterterm insertions, necessary for performing renormalization and computing the rational term \mathcal{R}_2 in the massive case.

We observe that in the limit in which terms suppressed by positive powers of the electron or muon mass are neglected, the contributions induced by ultraviolet counterterms and \mathcal{R}_2 -like rational terms can be embedded in the computation by means of simple factors that multiply the tree-level amplitude. By using the U(1) Ward identity in order to eliminate the charge counterterm, we find that the ultraviolet counterterm \mathcal{UV}_{ct} in Eq. (9) originates from

$$\mathcal{M}_{1\text{-loop}}[\mathcal{UV}_{ct}] = \mathcal{M}_{\text{tree}} \frac{\alpha}{4\pi} (2\delta\mathcal{Z}_\psi - \delta\mathcal{Z}_A), \quad (11)$$

where field counterterms are defined through $A_\mu = \mathcal{Z}_A^{1/2} A_\mu^R$, $\psi = \mathcal{Z}_\psi^{1/2} \psi^R$, $\mathcal{Z}_i = 1 + \alpha/(4\pi)\delta\mathcal{Z}_i$, with $i = A, \psi$, and the index R has been introduced for denoting renormalized quantities. Explicitly we have the well-known expressions

$$\begin{aligned} \delta\mathcal{Z}_\psi &= Q_f^2 \left[-3 \left(\frac{1}{\epsilon} - \gamma - \ln\pi \right) + 3 \ln \left(\frac{m_f^2}{\mu^2} \right) - 4 \right], \\ \delta\mathcal{Z}_A &= \frac{4}{3} \sum_f N_f Q_f^2 \left[-\frac{1}{\epsilon} + \gamma + \ln\pi + \ln \left(\frac{m_f^2}{\mu^2} \right) \right], \end{aligned} \quad (12)$$

where the index f runs over the fermions, N_f is the color factor ($N_f = 1$ for leptons and $N_f = 3$ for quarks), Q_f is the quantum number associated with the electric charge, m_f is the fermion mass, γ is the Euler-Mascheroni constant and μ is the 't Hooft mass. We used the same dimensional regulator for both ultraviolet and infrared divergencies.

Similarly, in the same limit, the \mathcal{R}_2 component in Eq. (9) arises from the interference of

$$\mathcal{M}_{1\text{-loop}}[\mathcal{R}_2] = \mathcal{M}_{\text{tree}} \frac{\alpha}{4\pi} \left(-5 + \frac{2}{3} \sum_f N_f Q_f^2 \right) \quad (13)$$

with the tree-level amplitude.

The common structure of those terms in the fully massive case suggests that the contributions to the rational term \mathcal{R}_2 can be fully combined with ultraviolet counterterms, thus achieving a significant optimization in this part of the calculation.

The cut-constructible term and the term \mathcal{R}_1 in Eq. (9) were obtained by applying the OPP method. Each step of the calculation was performed in two independent ways.

The first version employs the routines of the publicly available package CUTTOOLS [25], for determining numerically the coefficients which multiply the scalar integrals, combined with QCD-LOOP [29], used to evaluate the needed scalar integrals. The basis of loop integrals employed by CUTTOOLS involves rank-one and rank-two two-point functions, which in principle could be reduced to combinations of scalar bubbles and tadpoles, in order to improve the numerical stability; these tensor integrals have been included through the relations provided in Ref. [30].

The second version of our calculation, which we use in order to cross-check our results, makes use of an independent FORTRAN 95 code for the reduction of the tensor integrals, which includes an optional optimization for the OPP technique based on the Discrete Fourier Transform [31]. The basis integrals are evaluated using ONELOOP [32], written by A. van Hameren.

It is interesting to observe that the rational part \mathcal{R}_1 is computed by using different strategies in the two versions of the calculation: CUTTOOLS employs the mass-shift procedure introduced in [12], while the second approach uses the counterterm-based approach described in Ref. [13].

The results obtained with the two independent implementations for the cut-constructible term and the component \mathcal{R}_1 are in very good agreement.

A final comment concerns vacuum polarization insertions (such as diagram 2a in Fig. 2). Although these types of diagrams are implemented in both codes, they are naturally incorporated in any QED computation by simply running the fine-structure constant α to the appropriate scale. Furthermore, the introduction of a running fine-structure constant allows for a straightforward inclusion of hadronic contributions using dispersion relations and the optical theorem. Since this class of corrections is well-known, it will be neglected in the rest of the paper.

2.3 Real Soft-Photon Corrections

Real soft-photon corrections to the processes $e^-e^+ \rightarrow e^-e^+\gamma$ and $e^-e^+ \rightarrow \mu^-\mu^+\gamma$ can easily be obtained and are already implemented in Monte Carlo event generators.

In order to check our calculations, it is useful to compare the coefficients of the residual infrared poles for the virtual one-loop corrections with the analytic expressions of the corresponding poles arising from real soft-photon emission diagrams. In fact, the sum of the one-loop corrections to $e^-e^+ \rightarrow e^-e^+\gamma$ ($e^-e^+ \rightarrow \mu^-\mu^+\gamma$) and the real-emission diagrams for $e^-e^+ \rightarrow e^-e^+\gamma\gamma_{\text{soft}}$ ($e^-e^+ \rightarrow \mu^-\mu^+\gamma\gamma_{\text{soft}}$) is infrared finite after integration over the soft-photon phase space up to a given upper cut-off on the energy of the undetected photon γ_{soft} .

The contribution of real soft-emission diagrams factors in the product of the LO cross section of Eq. (3) and an infrared-divergent coefficient which we take from Ref. [33],

$$d\sigma_{\text{NLO}}^{\text{R}} = \frac{\alpha}{\pi} d\sigma_{\text{LO}} \left(\frac{1}{\epsilon} \sum_{i,j=1}^4 J_{ij} + \Delta J_{ij} \right), \quad (14)$$

where the infrared-divergent terms J_{ij} can be written in the compact form

$$J_{ij} = \frac{\varepsilon_i \varepsilon_j}{4\beta_{ij}} \ln \left(\frac{1 + \beta_{ij}}{1 - \beta_{ij}} \right), \quad \text{with} \quad \beta_{ij} = \sqrt{1 - \frac{m_i^2 m_j^2}{(k_i \cdot k_j)^2}}, \quad (15)$$

and ΔJ_{ij} is a finite remainder which we do not consider in the present work. Here we have introduced $\varepsilon_i = 1$ for $i = 1, 4$ and $\varepsilon_i = -1$ for $i = 2, 3$. The case $i = j$ can be obtained by taking the limit $\beta_{ij} \rightarrow 0$ in Eq. (15); one finds

$$J_{ii} = \frac{1}{2}. \quad (16)$$

3 Numerical Results

In this section we show numerical results for the squared LO amplitude, summed and averaged over the spins, and the associated one-loop virtual corrections (excluding trivial vacuum polarization corrections) for both processes at fixed phase space points. We define

$$\frac{1}{4} \sum_{\text{spins}} |\mathcal{M}_{\text{tree}}|^2 = \mathcal{I}_{\text{LO}}, \quad \frac{1}{4} \sum_{\text{spins}} 2 \operatorname{Re} (\mathcal{M}_{1\text{-loop}} \mathcal{M}_{\text{tree}}^*) = (e^\gamma \pi)^{-\epsilon} \mathcal{I}_{\text{NLO}}^V, \quad (17)$$

where $\gamma = 0.5772156 \dots$ and we have set for definiteness the arbitrary 't Hooft mass unit to the value $\mu = 1$ GeV. Following Eq. (9), we further define

$$\mathcal{I}_{\text{NLO}}^V = \mathcal{I}_{\text{NLO}}^V(\mathcal{CC}_4 + \mathcal{R}_1 + \mathcal{R}_2) + \mathcal{I}_{\text{NLO}}^V(\mathcal{UV}_{ct}), \quad (18)$$

isolating the contribution of the ultraviolet counterterms from the sum of the cut-constructible and rational parts.

3.1 Results for $e^-e^+ \rightarrow \mu^-\mu^+\gamma$

As an example of our results for the process $e^-e^+ \rightarrow \mu^-\mu^+\gamma$, we set $\sqrt{s} = 10$ GeV and show the values for the following phase space point:

$$\begin{aligned} k_1 &= (5, 0, 4.9999999738880110, 0), \\ k_2 &= (5, 0, -4.9999999738880110, 0), \\ k_3 &= (0.57385779257979530, 0.45500969957902548, -0.33152175208505869, 3.47645907628224629 \cdot 10^{-2}), \\ k_4 &= (4.9478976170272837, -1.9887465557319073, 4.2444753589966897, -1.5810892454259360), \\ k_5 &= (4.4782445903929213, 1.5337368561528819, -3.9129536069116311, 1.5463246546631135), \end{aligned} \quad (19)$$

where $k_i = (k_i^0, k_i^1, k_i^2, k_i^3)$ and all quantities are expressed in GeV. After splitting the one-loop corrections according to Eq. (18), we obtain:

$$\begin{aligned} \mathcal{I}_{\text{LO}} &= +5.01396482592499949 \cdot 10^{-3}, \\ \mathcal{I}_{\text{NLO}}^V(\mathcal{CC}_4 + \mathcal{R}_1 + \mathcal{R}_2) &= +\frac{1}{\epsilon} 3.66626587615940115 \cdot 10^{-4} + 1.94405539117213817 \cdot 10^{-3}, \\ \mathcal{I}_{\text{NLO}}^V(\mathcal{UV}_{ct}) &= -\frac{1}{\epsilon} 3.48191977673850488 \cdot 10^{-5} - 3.89224934043765969 \cdot 10^{-4}, \\ \mathcal{I}_{\text{NLO}}^V &= +\frac{1}{\epsilon} 3.31807389848555066 \cdot 10^{-4} + 1.55483045712837215 \cdot 10^{-3}, \\ \mathcal{I}_{\text{NLO}}^R &= -\frac{1}{\epsilon} 3.31807389694548050 \cdot 10^{-4}. \end{aligned} \quad (20)$$

All results are expressed in GeV^{-2} ; they have been obtained working in double precision and using the input data suggested by the Particle Data Book [34]. The last line of Eq. (20) refers to the

infrared pole for real soft-photon emission and is defined as

$$\mathcal{I}_{\text{NLO}}^{\text{R}} = \frac{\alpha}{\pi} \mathcal{I}_{\text{LO}} \frac{1}{\epsilon} \sum_{i,j=1}^4 J_{ij}, \quad (21)$$

with J_{ij} defined in Eq. (15).

In order to check the stability of the OPP reduction, we have performed the so-called $N = N$ test, controlling the agreement between the numerical values of the numerator function $\bar{N}(\bar{q})$ of Eq. (10) before and after the decomposition in terms of inverse propagators [25]. When the numerical agreement in the comparison does not reach a given limit set by the user, the code automatically triggers the use of the more time-consuming multi-precision routines [35]. We observe more than 9 digits of agreement between the results obtained in double precision, requiring a 10^{-5} relative precision for the $N = N$ test, and those we got after forcing multiprecision in the reduction program, in order to reach a 10^{-15} relative precision.

A second test on the precision of our calculation concerns the cancellation of the poles. After renormalization, the residual pole for $\mathcal{I}_{\text{NLO}}^{\text{V}}$ is of pure infrared origin and it matches the infrared pole in $\mathcal{I}_{\text{NLO}}^{\text{R}}$ with an agreement of 9 digits.

Finally, as stressed in Section 2.2, we have performed the calculation of all contributions by means of two independent codes in order to be confident on our results.

In order to show the stability of our results, we study the process $e^-e^+ \rightarrow \mu^-\mu^+\gamma$ for $\sqrt{s} = 1$ GeV and fix the momenta of the colliding leptons and the outgoing photon to be:

$$\begin{aligned} k_1 &= (0.5, 0, 0, 4999997388800458), \\ k_2 &= (0.5, 0, 0, -0.4999997388800458), \\ k_5 &= (0.4, 0.16476049929759706, -0.3568677260727233, 0.07415796625373612), \end{aligned} \quad (22)$$

with all momenta given in GeV. Next, we compute and plot in Fig. 4 the finite part of the virtual corrections, $\mathcal{I}_{\text{NLO}}^{\text{V}}$ of Eq. (17), as a function of the energy of the outgoing muon E_- , moving between two configurations where the muon momentum is (almost) parallel or antiparallel to the photon momentum and collinear divergencies show up.

3.2 Results for $e^-e^+ \rightarrow e^-e^+\gamma$

As an example for the process $e^-e^+ \rightarrow e^-e^+\gamma$, we present numerical results for the following phase space point at $\sqrt{s} = 1$ GeV:

$$\begin{aligned} k_1 &= (0.5, 0, 0.49999973888004579, 0), \\ k_2 &= (0.5, 0, -0.49999973888004579, 0), \\ k_3 &= (0.17809378475586005, -0.12791641809859033, 5.00680988409300393 \cdot 10^{-2}, -0.11334774152166457), \\ k_4 &= (0.35639444064573744, -2.86053064231987925 \cdot 10^{-2}, -0.18321427299490697, -0.30435341762281021), \\ k_5 &= (0.46551177459840243, 0.15652172452178909, 0.13314617415397695, 0.41770115914447481), \end{aligned} \quad (23)$$

with all quantities expressed in GeV. We obtain

$$\begin{aligned} \mathcal{I}_{\text{LO}} &= +0.75861014681036187, \\ \mathcal{I}_{\text{NLO}}^{\text{V}}(\mathcal{CC}_4 + \mathcal{R}_1 + \mathcal{R}_2) &= +\frac{1}{\epsilon} 4.74506427003504525 \cdot 10^{-2} + 0.50058282682639688, \\ \mathcal{I}_{\text{NLO}}^{\text{V}}(\mathcal{UV}_{ct}) &= -\frac{1}{\epsilon} 5.28634805094575690 \cdot 10^{-3} - 8.71804407858063207 \cdot 10^{-2}, \end{aligned}$$

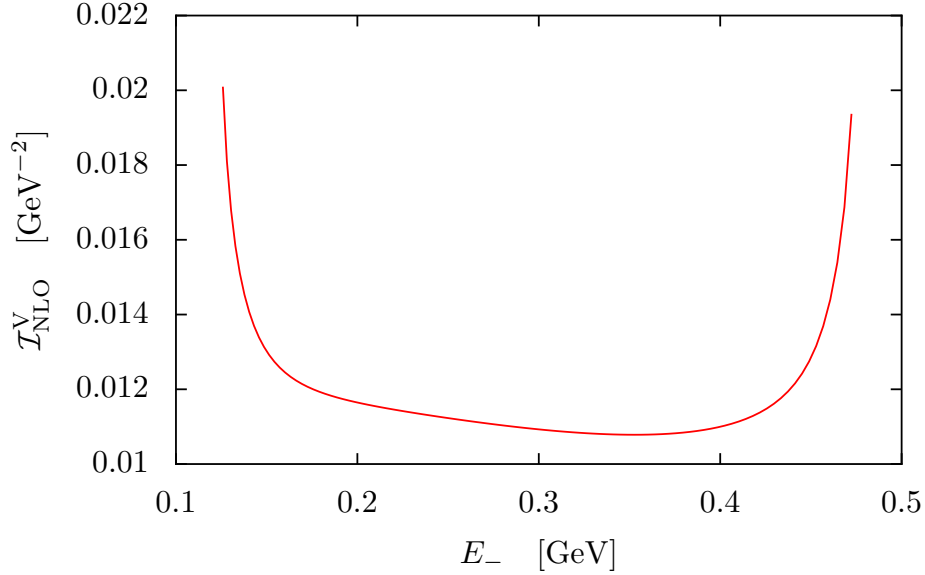


Figure 4: Virtual corrections for $e^-e^+ \rightarrow \mu^-\mu^+\gamma$ for $\sqrt{s} = 1$ GeV and $k_5^0 = 0.4$ GeV as a function of the energy of the outgoing muon.

$$\begin{aligned}\mathcal{I}_{\text{NLO}}^V &= +\frac{1}{\epsilon} 4.21642946494046947 \cdot 10^{-2} + 0.41340238604059049, \\ \mathcal{I}_{\text{NLO}}^R &= -\frac{1}{\epsilon} 4.21642946495862717 \cdot 10^{-2},\end{aligned}\tag{24}$$

where all results are expressed in GeV^{-2} . All numbers have been obtained working in double precision and requiring a 10^{-5} relative precision for the $N = N$ test. Also for this process, we have tested the precision of our calculations by forcing multiprecision in the reduction program, by comparing the two independent implementations, and finally by checking the complete cancellation of infrared and ultraviolet poles.

4 Conclusions

We have applied the OPP method to evaluate the complete NLO virtual QED corrections to hard-bremsstrahlung processes $e^-e^+ \rightarrow e^-e^+\gamma$ and $e^-e^+ \rightarrow \mu^-\mu^+\gamma$ relevant for determining the luminosity at low-energy electron-positron colliders.

It is interesting to note that in the case of muon pair production in association with a hard photon, the calculation has been performed retaining both the electron and muon masses: this shows once more the capability of the method in dealing with several scales inside the loop diagrams.

Concerning numerical stability, we have performed three different tests on our results: the cross-check between two independent codes, the complete cancellation of infrared and ultraviolet poles and the test on the reconstructed numerators. For leading order calculations, we find an agreement of at least 12 digits; for the NLO results, we have 9 digits of agreement.

In particular, the results of our calculation, both for Bhabha scattering and muon pair production, have been implemented in a FORTRAN 95 code which employs the publicly available

package CUTTOOLS for the extraction of the coefficients of the scalar integrals, combined with the package QCDLOOP, used to evaluate the needed scalar integrals.

The typical order of magnitude of the CPU time of the FORTRAN 95 code we have developed is $\mathcal{O}(10^{-1})$ seconds for each phase space point on a standard desktop machine. The computational speed, together with the modular approach we have followed in computing the radiative corrections, allows for an implementation of the results in the existing Monte Carlo programs.

The results we derived allows for a phenomenological study of the two hard-bremsstrahlung processes $e^-e^+ \rightarrow e^-e^+\gamma$ and $e^-e^+ \rightarrow \mu^-\mu^+\gamma$, including the calculation of the cross sections and the relevant distributions.

Acknowledgments

We thank A. Ferroglia for his invaluable help during all stages of the computation. We also thank S. Pozzorini for discussions and clarifications concerning the interplay between infrared poles and rational terms, R.K. Ellis and G. Zanderighi for useful communications concerning QCDLOOP and A. van Hameren for help with ONELOOP. Feynman diagrams have been drawn with the packages AXODRAW [36] and JAXODRAW [37].

The research of S.A. was supported by the Deutsche Forschungsgemeinschaft through Sonderforschungsbereich/Transregio 9 *Computergestützte Theoretische Teilchenphysik..* The work of G.O. was supported in part by the NSF Grant No. PHY-0855489.

References

- [1] C.M. Carloni Calame, C. Lunardini, G. Montagna, O. Nicrosini and F. Piccinini, Nucl. Phys. B **584** (2000) 459, arXiv:hep-ph/0003268;
C.M. Carloni Calame, Phys. Lett. B **520** (2001) 16, arXiv:hep-ph/0103117;
G. Balossini, C.M. Carloni Calame, G. Montagna, O. Nicrosini and F. Piccinini, Nucl. Phys. B **758** (2006) 227, arXiv:hep-ph/0607181.
- [2] A.B. Arbuzov, G.V. Fedotov, E.A. Kuraev, N.P. Merenkov, V.D. Rushai and L. Trentadue, JHEP **9710** (1997) 001, arXiv:hep-ph/9702262;
A.B. Arbuzov, G.V. Fedotov, F.V. Ignatov, E.A. Kuraev and A.L. Sibidanov, Eur. Phys. J. C **46** (2006) 689, arXiv:hep-ph/0504233.
- [3] S. Jadach, W. Placzek and B.F.L. Ward, Phys. Lett. B **390** (1997) 298, arXiv:hep-ph/9608412.
- [4] G. Balossini, C. Bignamini, C.M. Carloni Calame, G. Montagna, O. Nicrosini and F. Piccinini, Nucl. Phys. Proc. Suppl. **183** (2008) 168, arXiv:0806.4909 [hep-ph].
- [5] M. Consoli, Nucl. Phys. B **160** (1979) 208;
M. Böhm, A. Denner, W. Hollik and R. Sommer, Phys. Lett. B **144** (1984) 414.
- [6] R. Bonciani, A. Ferroglia, P. Mastrolia, E. Remiddi and J.J. van der Bij, Nucl. Phys. B **701** (2004) 121, arXiv:hep-ph/0405275; Nucl. Phys. B **716** (2005) 280, arXiv:hep-ph/0411321.
- [7] A.A. Penin, Phys. Rev. Lett. **95** (2005) 010408, arXiv:hep-ph/0501120; Nucl. Phys. B **734** (2006) 185, arXiv:hep-ph/0508127;
R. Bonciani and A. Ferroglia, Phys. Rev. D **72** (2005) 056004, arXiv:hep-ph/0507047.

- [8] T. Becher and K. Melnikov, JHEP **0706** (2007) 084, arXiv:0704.3582 [hep-ph];
S. Actis, M. Czakon, J. Gluza and T. Riemann, Nucl. Phys. B **786** (2007) 26, arXiv:0704.2400 [hep-ph].
- [9] S. Actis, M. Czakon, J. Gluza and T. Riemann, Phys. Rev. Lett. **100** (2008) 131602, arXiv:0711.3847 [hep-ph]; Phys. Rev. D **78** (2008) 085019, arXiv:0807.4691 [hep-ph];
R. Bonciani, A. Ferroglia and A.A. Penin, Phys. Rev. Lett. **100** (2008) 131601, arXiv:0710.4775 [hep-ph]; JHEP **0802** (2008) 080, arXiv:0802.2215 [hep-ph];
J.H. Kühn and S. Uccirati, Nucl. Phys. B **806** (2009) 300, arXiv:0807.1284 [hep-ph].
- [10] A.B. Arbuzov, V.S. Fadin, E.A. Kuraev, L.N. Lipatov, N.P. Merenkov and L. Trentadue, Nucl. Phys. B **485** (1997) 457, arXiv:hep-ph/9512344;
S. Jadach, M. Melles, B.F.L. Ward and S.A. Yost, Phys. Lett. B **377** (1996) 168, arXiv:hep-ph/9603248;
B.F.L. Ward, S. Jadach, M. Melles and S.A. Yost, Phys. Lett. B **450** (1999) 262, arXiv:hep-ph/9811245.
- [11] S. Jadach, M. Melles, B.F.L. Ward and S.A. Yost, Phys. Rev. D **65** (2002) 073030, arXiv:hep-ph/0109279;
H. Czyż, A. Grzelinska, J.H. Kühn and G. Rodrigo, Eur. Phys. J. C **33** (2004) 333, arXiv:hep-ph/0308312.
- [12] G. Ossola, C.G. Papadopoulos and R. Pittau, Nucl. Phys. B **763** (2007) 147, arXiv:hep-ph/0609007.
- [13] G. Ossola, C.G. Papadopoulos and R. Pittau, JHEP **0707** (2007) 085, arXiv:0704.1271 [hep-ph].
- [14] F. del Aguila and R. Pittau, JHEP **0407** (2004) 017, arXiv:hep-ph/0404120.
- [15] H. Czyż, A. Grzelinska, J.H. Kühn and G. Rodrigo, Eur. Phys. J. C **39** (2005) 411, arXiv:hep-ph/0404078.
- [16] S.M. Swanson, Phys. Rev. **154** (1967) 1601;
A.C. Hearn, P.K. Kuo and D.R. Yennie, Phys. Rev. **187** (1969) 1950.
- [17] F.A. Berends, R. Kleiss, P. De Causmaecker, R. Gastmans and T.T. Wu, Phys. Lett. B **103** (1981) 124.
- [18] P. Nogueira, J. Comput. Phys. **105** (1993) 279.
- [19] G. 't Hooft and M.J.G. Veltman, Nucl. Phys. B **153** (1979) 365.
- [20] G. Passarino and M.J.G. Veltman, Nucl. Phys. B **160** (1979) 151.
- [21] Z. Bern *et al.*, arXiv:0803.0494 [hep-ph].
- [22] A. Bredenstein, A. Denner, S. Dittmaier and S. Pozzorini, Phys. Rev. Lett. **103** (2009) 012002, arXiv:0905.0110 [hep-ph];
G. Bevilacqua, M. Czakon, C.G. Papadopoulos, R. Pittau and M. Worek, arXiv:0907.4723 [hep-ph].

- [23] R.K. Ellis, K. Melnikov and G. Zanderighi, arXiv:0906.1445 [hep-ph];
C.F. Berger, Z. Bern, L.J. Dixon, F. Febres Cordero, D. Forde, T. Gleisberg, H. Ita, D.A. Kosower and D. Maitre, arXiv:0907.1984 [hep-ph].
- [24] J.A.M. Vermaseren, arXiv:math-ph/0010025.
- [25] G. Ossola, C.G. Papadopoulos and R. Pittau, JHEP **0803** (2008) 042, arXiv:0711.3596 [hep-ph].
- [26] RED, unpublished.
- [27] G. Ossola, C.G. Papadopoulos and R. Pittau, JHEP **0805** (2008) 004, arXiv:0802.1876 [hep-ph].
- [28] A. Bredenstein, A. Denner, S. Dittmaier and S. Pozzorini, JHEP **0808** (2008) 108, arXiv:0807.1248 [hep-ph].
- [29] R.K. Ellis and G. Zanderighi, JHEP **0802** (2008) 002, arXiv:0712.1851 [hep-ph];
G.J. van Oldenborgh, Comput. Phys. Commun. **66** (1991) 1.
- [30] A. Denner and S. Dittmaier, Nucl. Phys. B **734** (2006) 62, arXiv:hep-ph/0509141.
- [31] P. Mastrolia, G. Ossola, C.G. Papadopoulos and R. Pittau, JHEP **0806** (2008) 030, arXiv:0803.3964 [hep-ph].
- [32] A. van Hameren, C.G. Papadopoulos and R. Pittau, arXiv:0903.4665 [hep-ph];
A. van Hameren, J. Vollinga and S. Weinzierl, Eur. Phys. J. C **41** (2005) 361, arXiv:hep-ph/0502165.
- [33] D.Y. Bardin and G. Passarino, *The Standard Model in the making*, Oxford University Press, 1999.
- [34] C. Amsler *et al.* (Particle Data Group), Phys. Lett. B **667** (2008) 1.
- [35] D.H. Bailey, ACM Transactions on Mathematical Software, vol. 21, no.4 (1995) 379.
- [36] J.A.M. Vermaseren, Comput. Phys. Commun. **83** (1994) 45.
- [37] D. Binosi and L. Theussl, Comput. Phys. Commun. **161** (2004) 76, hep-ph/0309015.